Stagger tuned cMUT array for wideband airborne applications

Selim Olcum, Abdullah Atalar, Hayrettin Köymen and Muhammed N. Senlik
Dept. of Electrical and Electronics Engineering
Bilkent University
Ankara, Turkey 06800
Email: selim@ee.bilkent.edu.tr

***Abstract*— In this study, we explore the limits of cMUTs in air-borne applications. First we investigate the ways of increasing the bandwidth of a single cMUT cell in air. The effect of array operation is also considered in order to increase the radiation resistance seen by the transducer. We calculate the bandwidth of a stagger tuned cMUT array. It is shown in this paper that more than 60% bandwidth can be obtained by three staggered frequencies.**

I. Introduction

Capacitive micromachined ultrasonic transducer (cMUT) is a promising candidate for wideband applications in fluid media. For airborne applications where medium's loading is very small, cMUTs operate with a high quality factor. Hence the operation in the air is narrowband. Even though cMUTs provide a better impedance match to the fluid media than their piezoelectric counterparts, the impedance mismatch of a cMUT to air is still high.

Previously, the stagger tuned transducer arrays were proposed to increase the bandwidth of immersion cMUTs [1]. In order to provide a wideband operation in air, we propose the stagger tuned cMUT arrays as well. Since the center frequency of a cMUT element depends on its radial size, a wideband operation is possible when different sized cMUTs are connected in parallel.

II. Air Transducer Model

In this paper, the analysis of cMUTs is based on the method developed in [2] where Mason's equivalent circuit model is used. In Fig. 1a, the circuit model includes the loading of the immersion medium on the membrane and the reactive part of the radiation impedance. The inductor, L is the effective mass of the medium acting on the membrane. In the case of air-borne applications, the loading effect of the air on the membrane is minimum [3]. In this work, the effect of the air loading is ignored, therefore the equivalent circuit reduces as in Fig. 1b. In addition, the reactive part of the radiation impedance is ignored compared to the relatively larger mass of the membrane.

The shunt input capacitance, C is calculated using the parallel plate approximation ignoring the effect of fringing fields. The transformer ratio, n is calculated using the finite element method (FEM)[1] simulations. The mechanical impedance of the membrane, Z_m, is the Mason's mechanical impedance as given in Eq. 1.

$$Z_m = \frac{jw\rho t_m a k_1 k_2 (k_1 J_{10} - k_2 J_{01})}{a k_1 k_2 (k_1 J_{10} - k_2 J_{01}) - 2(k_1^2 + k_2^2) J_{11}} \quad (1)$$

where ω is the radian frequency, $J_{01} = J_0(k_1 a) J_1(k_2 a)$, $J_{10} = J_1(k_1 a) J_0(k_2 a)$ and $J_{11} = J_1(k_1 a) J_1(k_2 a)$. J_0 and J_1 are the zeroth and first-order Bessel functions of the first kind. k_1 and k_2 are given by

$$k_1 = \sqrt{\frac{\sqrt{d^2 + 4c\omega^2} - d}{2c}} \quad \text{and} \quad k_2 = \sqrt{\frac{\sqrt{d^2 + 4c\omega^2} + d}{2c}} \quad (2)$$

where

$$c = \frac{(Y_0 + T) t_m^2}{12 \rho_m (1 - \sigma^2)} \quad \text{and} \quad d = \frac{T}{\rho_m} \quad (3)$$

Y_0 is the Young's modulus, T is the residual stress[2], P is the applied pressure, σ is the Poisson's ratio and ρ_m is the density of the membrane material.

The expression in Eq. 1 is accurate as long as the thin plate approximation holds [4]. As we will shortly stress, in the case of air-coupled transducers higher a/t_m ratios generate higher bandwidths. Therefore the transducers considered in this work are suitable for thin plate approximation.

In the previous studies, the radiation impedance of the medium seen by the transducers, Z_a, is taken to be real and constant [5]. It is defined as the product of the density

[1]Simulations are done with ANSYS, ANSYS INC.,Canonsburg, PA.

[2]Since T is much smaller than Y_0, it is assumed to be zero.

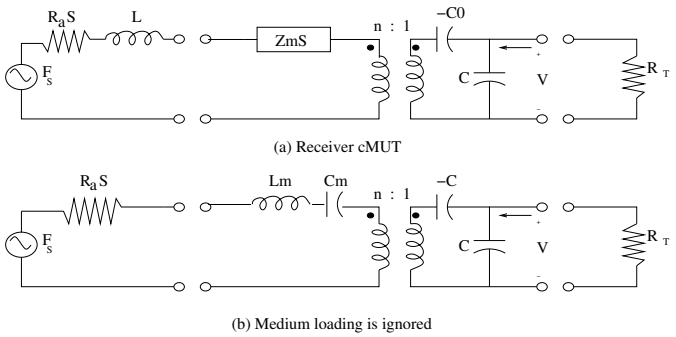

Fig. 1. (a) Mason's equivalent circuit model for receiver mode cMUT including medium's loading effect. (b) Medium's loading is ignored.

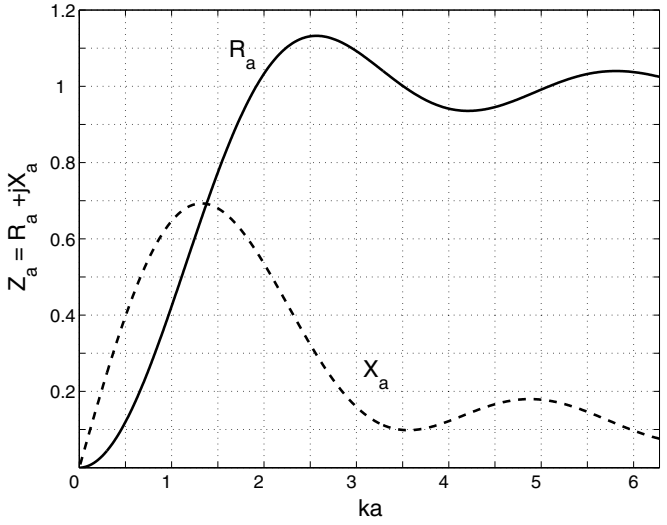

Fig. 2. Real (solid) and imaginary (dashed) parts of the radiation impedance seen by a circular piston transducer. Note that the curves are normalized to $S\rho_a c_a$.

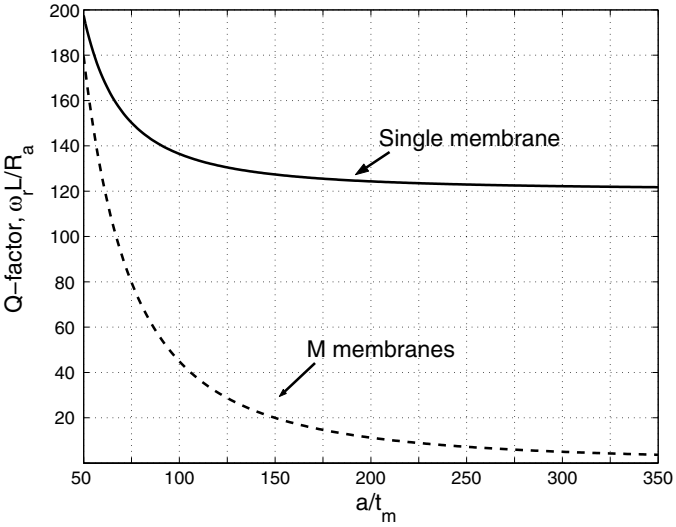

Fig. 3. Determination of Q-factor for different a/t_m values. The radiation impedance seen by a single cell transducer (solid line) and seen by a large enough array transducer so that $1 - 2J_1(ka)/(2ka) = 1$ (dashed line). Note that the curve is independent of individual values of a or t_m.

of medium and the velocity of sound in that medium. The radiation impedance of the medium seen by a circular piston transducer can be written as a function of the product of wavenumber and the effective aperture of the transducer [6]:

$$R_a = S\rho_a c_a \left(1 - 2\frac{J_1(2ka)}{2ka}\right) \tag{4}$$

where ρ_a is the density of air, c_a is the velocity of the sound in air, k is the wavenumber, S and a are the area and the radius of the circular piston. We plotted the real (R_a) and imaginary (X_a) parts of the radiation impedance seen by a circular piston transducer in Fig. 2. Note that the imaginary part is negligible compared to the mass of the membrane.

In what follows we try to maximize the bandwidth of the air-coupled transducers. We would like to start with transducers with a small Q-factor. The mechanical impedance of the membrane can be modelled by a series inductor-capacitor pair near the mechanical resonance of the membrane. If the transducers are high-Q, the bandwidth of the device can be predicted accurately using the series RLC circuit at the mechanical port of the Mason's equivalent circuit. For a series RLC network, Q-factor is determined by $Q = \omega_r L_m / R_a S$, where ω_r is the radian mechanical resonance frequency and L represents the effective mass of the membrane, $L_m = 1.883 \times \rho_m \pi a^2 {t_m}^3$. In Fig. 3, the Q-factor of a single cell transducer can be seen (solid-line) as a function of the a/t_m ratio. Note that Fig. 3 is independent of the individual values of the radius or the thickness of the membrane. We see from this figure that a thinner and larger membrane generates a lower-Q device.

In order to obtain higher radiated energies, cMUTs are fabricated as array transducers [**?**]. Such transducers have higher effective aperture. For example, if the number of cells in the transducer is chosen such that the normalized real part of the radiation impedance in Fig. 4 is maximum, the Q-factor can be decreased further. This effect is seen in the dashed-line of Fig. 3.

Using the above analysis, we can determine the bandwidth of the equivalent circuit. For a fixed resonance frequency, along the a-t_m pairs, the ones with the minimum thickness has the maximum a/t_m ratio, since the resonance frequency of the membrane is proportional to t_m/a^2. Choosing a thickness of 0.5 μm for a 100 KHz transducer corresponds to a cell with 148 μm radius. If we use 107 cells in the array, the radiation impedance per cell is maximized. In Fig. 4, the transducer gain of the device is given. Another transducer with a lower a/t_m ratio is also depicted in the same figure. The bandwidth is reduced in this case.

In what follows, we will investigate the techniques of achieving an even higher bandwidth from cMUTs coupled to air. The approach is to use different sized cells with different resonance frequencies in the same transducer array [7].

III. Stagger Tuned Transducers

In this section, we use stagger tuned cells in the same element. Due to ease of fabrication and batch processing purposes, we keep the vertical dimensions fixed for all the membranes on the wafer. The controlling parameters are the membrane radius and the electrode metallization radius. As a starting point, we assume the same percentage of the collapse voltage applied on each transducer, which is 90%. We consider full electrode coverage on the membranes. Therefore, the only controlling parameter will be the radii of the membranes, a.

In the following part, we will investigate the effect of the membrane radius on the circuit parameters in Fig. 1.

[3]The reactive part of the radiation impedance, X_a is ignored in comparison to this inductor.

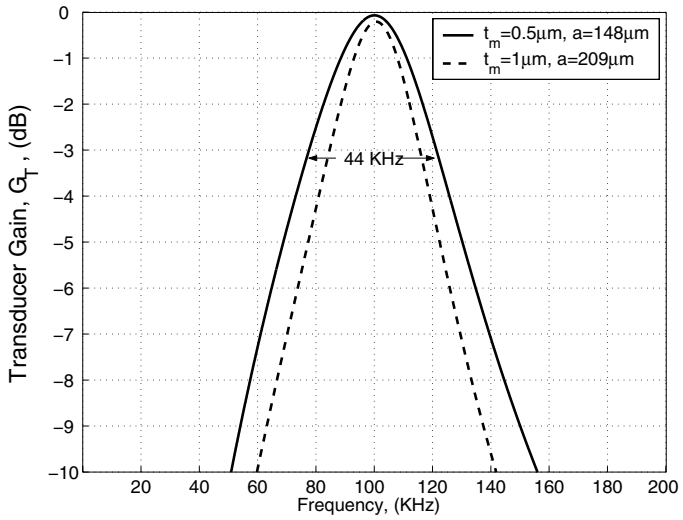

Fig. 4. Transducer gain of a single cMUT array for two different transducers. The one with a higher a/t_m has a larger bandwidth

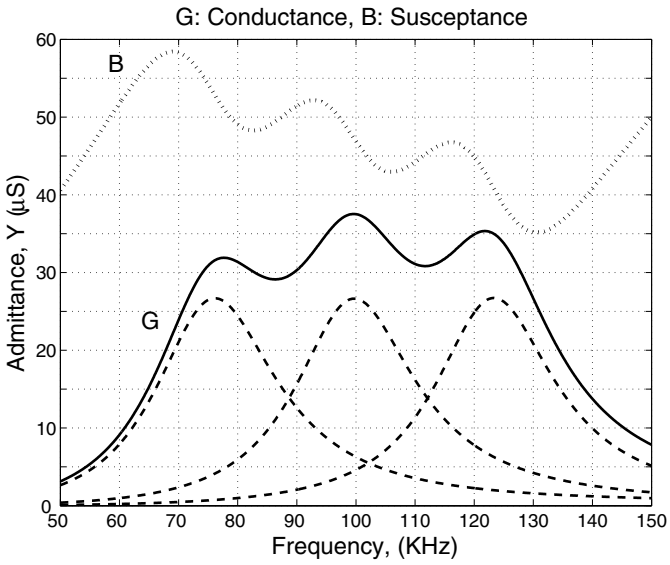

Fig. 5. Individual conductance curves of three different transducer elements, along with a stagger tuned transducer. The radii of individual cMUTs are 127μm, 141μm and 162μm. The membrane thickness is 0.5μm for all membranes.

1) Collapse Voltage, V_{col}: The approximate analytical expression for the collapse voltage of a fully metallized cMUT membrane is calculated in [2] as:

$$V_{col} \simeq 0.7\sqrt{\frac{128(Y_0+T)t_m^3\bar{t_g^3}}{27\epsilon_0(1-\sigma^2)a^4}} \tag{5}$$

Therefore, the collapse voltage of a cMUT cell is proportional to $1/a^2$. Note that all the other parameters are fixed on the same wafer.

2) Turns ratio, n: In the previous studies, the analytical expression for the turns ratio is obtained using the product of electrical field and input capacitance of the cMUT cell [2], [5]. Although this approach is not accurate enough, we will use it to understand the response of turns ratio value to the changes in membrane radius, a. Hence the turns ratio is:

$$n \propto C_0E = \frac{\epsilon_0\pi a^2V_{DC}}{\bar{t_g}^2} = 0.7\times 0.9\pi\sqrt{\frac{128\epsilon_0(Y_0+T)t_m^3}{27(1-\sigma^2)\bar{t_g}}} \tag{6}$$

which is independent of a. Therefore, all fully metallized transducer cells on the wafer have the same turns ratio, provided that they are driven at the same percentage of the collapse voltage. This behavior is also verified using FEM simulations.

3) Radiation resistance, R_a: The number of cells in a transducer element is adjusted such that R_a is maximum according to Eq. 2. The area of the element is $M\times\pi a^2$, where M is the number of cells. Assuming the transducer element is circular, the effective aperture radius, A is $\sqrt{M}a$. Using Fig. 2, for R_a is to be maximum ka should be equal to 2.58:

$$kA = \frac{2\pi f_r}{c}\sqrt{M}a = \text{constant} \Rightarrow \tag{7}$$

$$M \propto \frac{1}{f_r^2a^2} \propto \frac{1}{\frac{1}{a^4}a^2} \propto a^2 \tag{8}$$

Hence, the number of cells in an element is proportional to a^2. For a transducer element the conductance seen at the input port is R_aS/n^2. Since M number of cells will be connected in parallel, the conductance is R_aS/Mn^2. Recall that for different sized cells, the value of R_a and n are constant. Since M and S are both proportional to a^2, the maximum conductance for transducers with different sized cells is independent of the radius of the membrane. In Fig. 5, three different elements with different sized cells are demonstrated.

The fractional bandwidth of an element is approximately $1/Q$. We take the separation between the staggered resonance frequencies as $f_2-f_1=1/Q$, where f_1 and f_2 are resonance frequencies of adjacent transducers. The radii for the cells of three elements are 127μm, 141μm and 162μm, respectively. Note that the thickness for all the transducers are taken to be same and 0.5μm. As it is seen in Fig. 5, the stagger tuned array has more than 60% bandwidth in air. However, this bandwidth is not an upper limitation. Using more transducers elements with different cell radii further increases the bandwidth.

IV. Discussion and Conclusions

In this study we present a way of obtaining large bandwidths using stagger tuned cMUT arrays in air. We base our study on a few assumptions: we ignore the effect of the mass loading of the medium, since air is a very light medium. In addition, we ignore the imaginary part of the radiation impedance compared to the mass of the membrane.

We show that the bandwidth of a cMUT in air can be improved by increasing the a/t_m ratio of the membrane. In order to achieve larger bandwidths for the same resonance frequency, the membrane size must be kept small. The main parameter to be adjusted to obtain a higher bandwidth is the thickness of the membrane. We can obtain a larger bandwidth

using a thinner membrane with the same resonance frequency. However, in order to use acceptable bias voltages we use reasonable membrane thicknesses.

The effect of the transducer size is also considered. In order that the transducer to see a high radiation resistance, the aperture size must be large enough. Therefore, we increase the number of cMUT cells in the transducer element, to obtain a larger aperture size. This increases the bandwidth of the transducer further.

It is shown that the transformer ratio of a cMUT array is independent of the membrane radius provided that the membranes are biased at the same operating point. Since the transformation ratio and radiation impedance values are constant for membranes with different radii, the frequency response of the transducers is shifted.

One disadvantage of this approach is, the necessity of different operating voltages for different sized elements. That is a sacrifice in order to achieve constant turns ratio and radiation resistance values for different elements. One way of equating the collapse voltages is changing the electrode coverage. However, with this approach the transformer ratio values are not constant for different elements.

In a stagger tuned array, every cell transmits in a small frequency range efficiently, such that when combined, a wide band operation is possible. This results in a decrease in the maximum power handling capacity of the array, when compared to an ideal transducer array of the same aperture. In the receive mode of operation, the fact that the sound pressure at every frequency is intercepted by only a fraction of cMUT elements in the array, results in a proportional gain drop.

V. Acknowledgments

We would like to acknowledge the financial support of The Scientific and Technological Research Council of Turkey (TÜBİTAK) through the research grant EEEAG#105E023.

References

[1] C. Bayram, S. Olcum, M. N. Senlik, and A. Atalar, "Bandwidth improvement in a cMUT array with mixed sized elements," in Proc. of 2005 Ultrasonics Symposium, 2005.

[2] S. Olcum, M. N. Senlik, and A. Atalar, "Optimization of the gain-bandwidth product of capacitive micromachined ultrasonic transducers," IEEE Trans. Ultrason., Ferroelect., Freq. Contr., vol. 52, pp. 2211–2219, 2005.

[3] I. Ladabaum, X. C. Jin, and B. T. Khuri-Yahub, "Miniature drumheads: microfabricated ultrasonic transducers," Ultr., vol. 36, pp. 25–29, 1998.

[4] W. Mason, Electromechanical Transducers and Wave Filters. Van Nostrand, New York, 1942.

[5] A. Lohfink and P.-C. Eccardt, "Linear and nonlinear equivalent circuit modelling of CMUTs," IEEE Trans. Ultrason., Ferroelect., Freq. Contr., vol. 52, pp. 2163–2172, 2005.

[6] P. Morse and K. Ingard, Theoretical Acoustics. Princeton NJ: Princeton University Press, 1986.

[7] Y. Zhang, Q. Chen, X. Zang, and Z. Hou, "A wide-band stagger-tuned transducer used for pulsed ultrasonic doppler flowmeter," in Proc. of 1989 Eng. Med. in Bio. Soc., pp. 1110–1111, 1989.